Use of internal scintillator radioactivity to calibrate DOI function of a PET detector with a dual-ended-scintillator readout

Chad Bircher and Yiping Shao[a)]
Department of Imaging Physics, The University of Texas MD Anderson Cancer Center, Houston, Texas 77030

(Received 22 August 2011; revised 21 December 2011; accepted for publication 22 December 2011; published 18 January 2012)

Purpose: Positron emission tomography (PET) detectors that use a dual-ended-scintillator readout to measure depth-of-interaction (DOI) must have an accurate DOI function to provide the relationship between DOI and signal ratios to be used for detector calibration and recalibration. In a previous study, the authors used a novel and simple method to accurately and quickly measure DOI function by irradiating the detector with an external uniform flood source; however, as a practical concern, implementing external uniform flood sources in an assembled PET system is technically challenging and expensive. In the current study, therefore, the authors investigated whether the same method could be used to acquire DOI function from scintillator-generated (i.e., internal) radiation. The authors also developed a method for calibrating the energy scale necessary to select the events within the desired energy window.
Methods: The authors measured the DOI function of a PET detector with lutetium yttrium orthosilicate (LYSO) scintillators. Radiation events originating from the scintillators' internal Lu-176 beta decay were used to measure DOI functions which were then compared with those measured from both an external uniform flood source and an electronically collimated external point source. The authors conducted these studies with several scintillators of differing geometries (1.5×1.5 and 2.0×2.0 mm^2 cross-section area and 20, 30, and 40 mm length) and various surface finishes (mirror-finishing, saw-cut rough, and other finishes in between), and in a prototype array.
Results: All measured results using internal and external radiation sources showed excellent agreement in DOI function measurement. The mean difference among DOI values for all scintillators measured from internal and external radiation sources was less than 1.0 mm for different scintillator geometries and various surface finishes.
Conclusions: The internal radioactivity of LYSO scintillators can be used to accurately measure DOI function in PET detectors, regardless of scintillator geometry or surface finish. Because an external radiation source is not needed, this method of DOI function measurement can be practically applied to individual PET detectors as well as assembled systems. [DOI: 10.1118/1.3676688]

Key words: positron emission tomography, detector, depth of interaction, internal scintillator radioactivity, solid-state photomultiplier

I. INTRODUCTION

In a previous study, we evaluated a novel method to calibrate the depth-of-interaction (DOI) function of a positron emission tomography (PET) detector that applies a dual-ended-scintillator readout.[1] This method, which uses a simple setup and requires a single measurement, can be used to accurately and consistently calibrate the DOI function. The method also requires that an external flood radiation source irradiate a scintillator uniformly across its depth. In principle, however, the method could also be applied to scintillators that have natural internal radioactivity, such as lutetium oxyorthosilicate (LSO) and lutetium yttrium oxyorthosilicate (LYSO), if the distribution of internal radiation positions is known. Such a method could not only simplify the calibration process but also be applied to detectors within PET systems, where using an external uniform flood radiation source is typically difficult and expensive.

Because of its short decay time, high stopping power, and light yield, LSO and LYSO have become the scintillator materials of choice for all time-of-flight and many nontime-of-flight PET detectors.[2,3] LYSO contains a fraction of Lu-176 (~2.6% abundance), a natural radioactive element with a half-life of $\sim 3.8 \times 10^{10}$ years.[4,5] The energies of the main prompt gamma rays emitted from this nuclide are 88, 202, and 307 keV. In addition, the energy spectrum of internal LYSO interactions shows a strong continuous background from internal beta decays. The endpoint energy of most beta decays is 597 keV, which overlaps with the 511-keV gamma rays emitted from the PET radiotracers. In the current study, we compared DOI function measurements acquired using internal radioactivity from several LYSO scintillators with DOI function measurements acquired using external source methods, including using an electronically collimated external Na-22 point source to determine the interaction positions for DOI measurement.[6] We also assessed the impact of scintillator geometry and surface finish on the accuracy of DOI function measurement and investigated whether calibrating the energy scale and applying an energy filter to the acquired internal radiation improved the accuracy of DOI function measurement.

In addition, to further evaluate the new method to calibrate DOI function with all factors that could impact the DOI measurement, we have developed a practical PET detector consisting of an array of LYSO scintillators with dual-ended readout and compared DOI functions of scintillators in the array calibrated from each of the three different methods. This study should directly address the question of whether this new method can be accurately applied to a practical PET detector.

II. MATERIALS AND METHODS

II.A. Experiment setup and measurement

Two experimental setups were used for the study: (1) With the exception of photomultiplier choice, the experimental setup we used for a single scintillator study was identical to that used in our previous study.[1] Briefly, an LYSO crystal was directly coupled to two solid-state photomultipliers (SSPMs; model SPMArray2, SensL Technologies Ltd., Cork, Ireland) from both ends using optical grease, but without light sharing (Fig. 1).[7] LYSO scintillators of different sizes and surface finishes were prepared and evaluated (Table I). Besides the saw-cut surface finishes, surface finishes were prepared by polishing the scintillators with lapping films of corresponding finishing grades. To improve light output, we wrapped the scintillators' four axial sides with white Teflon tape.[8–12] (2) An 8×8 array of LYSO scintillators was constructed and used to validate the new method to calibrate the DOI function beyond a single crystal. Each scintillator has size of $1.9 \times 1.9 \times 30$ mm^3, with saw-cut surface finish and optically separated from other scintillators on all sides except two ends by ESR reflectors [3M (Ref. 13)]. The overall size of the array is $\sim 16 \times 16 \times 30$ mm^3. Each end of the scintillator array was optically coupled to one SSPM array through a light guide for improving the light sharing of photons from one scintillator to multiple SSPMs. The ESR is glued to the LYSO on two sides, and coupled with an air gap on the other two sides. The scintillator, optical guide, and SSPM arrays are glued together, which gives stability between measurements.

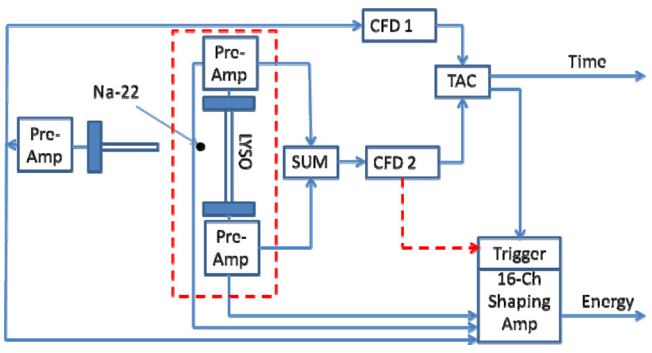

FIG. 1. A schematic of the dual-ended-scintillator readout and experiment setup for DOI function measurement. An LYSO scintillator was read out by two SSPMs from two ends for the DOI function measurement with internal or external radiation. An external Na-22 point source was used for external radiation measurement. During external flood source measurements the TAC was bypassed and only the signals from the SSPM's attached to the test crystal were digitized.

TABLE I. Geometries and surface finishes of scintillators used.

Scintillator size, mm	Surface finish, μm
$1.5 \times 1.5 \times 20$	Saw-cut
$1.5 \times 1.5 \times 20$	12
$1.5 \times 1.5 \times 20$	9
$1.5 \times 1.5 \times 20$	5
$1.5 \times 1.5 \times 30$	Saw-cut
$2.0 \times 2.0 \times 20$	Saw-cut
$2.0 \times 2.0 \times 20$	12
$2.0 \times 2.0 \times 20$	9
$2.0 \times 2.0 \times 20$	5
$2.0 \times 2.0 \times 30$	Saw-cut
$2.0 \times 2.0 \times 40$	Saw-cut

II.B. Validation of DOI measurement using an external radiation source

We placed a Na-22 point source ($\sim$1.0-mm diameter) $\sim$14 cm from the detector to mimic uniform radiation across the detector depth with the same SSPM bias and all other operation conditions. Photo-peak positions were used to scale the energy at different DOI positions.

We also used a step-and-shoot method to measure DOI. This approach consisted of a Na-22 point source and a second detector comprising a $0.5 \times 1.0 \times 5.0$ mm^3 LYSO crystal optically coupled to a single-channel photomultiplier (model R7400, Hamamatsu Corp, Japan) for the single pixel studies. The DOI positions were determined by electronically collimating coincidence events between the primary and the secondary detectors (Fig. 1). The Na-22 point source and the secondary detector stepped over in 1.0 mm distance increments along the axial length of the primary detector. Signals from both SSPMs at each DOI position were acquired and summed with equal electronic gains. The same low-level signal threshold, as used to measure internal radiation, was used to trigger summed signal during these acquisitions. The uncertainty of DOI positioning by this method was estimated about 1.8 mm. The setup for the array was similar with the exception that the photodetectors on the array and the collimation crystal were SSPM arrays, and the collimated beam width was approximately 2–3 mm depending on the interaction position between entrance crystal and exit crystal from the external beam.

For a single scintillator measurement, the above two DOI function measurements from external sources required

TABLE II. Solid-state photomultiplier specifications.

Parameters	Specifications
Pixel sensitive area	2.85×2.85 mm^2
Pixel size	3.0×3.0 mm^2
Pixel pitch	3.2 mm
No. of microcells	3640
Breakdown voltage	$\sim$27.5 V
Typical gain	10^6
Array matrix	4×4

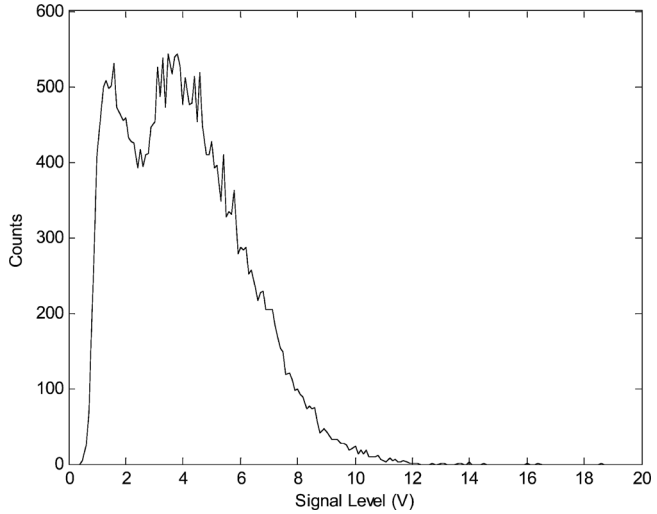

FIG. 2. Measured energy spectrum of the internal radiation of an LYSO scintillator.

different setups and different experiment processes, and they were usually conducted at different times mainly because the optical grease applied between the scintillator and SSPM arrays dried after a lengthy measurement and needed replacement. Therefore, the detector operating conditions, including the biases, gains, optical coupling efficiency, and signal threshold levels of the SSPMs, were usually different. This makes it difficult to compare the results from two methods with external sources. However, the data measured from the internal source were acquired immediately after each external measurement so that the DOI functions measured from the internal and external sources could be compared in pair with the same detector operating and data acquisition conditions. The stability issues are eliminated in the DOI array setup, and so measurements taken at different times may be compared directly.

II.C. SSPM arrays

The device characteristics and performance specifications of the SSPM arrays are summarized in Table II. For single scintillator measurements, each end of the scintillator was optically coupled to one SSPM within its pixel size (3×3 mm^2) to prevent light loss and optical crosstalk. The signals from the two SSPM pixels were amplified through custom-made preamplifiers that were based on operational amplifiers (AD8066). A nominal –32 V bias was applied to both SSPMs, resulting in an intrinsic amplification gain of close to 10^6. For scintillator array measurement, signals from all SSPM pixels were read out and processed with a custom made ASIC electronics and data acquisition.[14,15]

II.D. Data acquisition for single scintillator measurements

Conventional NIM and CAMAC electronics were used for data acquisition in the single crystal measurements (Fig. 1). Signals from each SSPM were sent to a 16-channel shaping amplifier (model N568LC, CAEN, Italy). An analog-to-digital converter (model PCI-416, Datel, USA) was used to digitize amplitude values. The DOI function and other measured values were calculated on the basis of these signal amplitudes. We acquired coincident events between the primary detector and the secondary detector for experiments using the step-and-shoot method (external collimated radiation source). Signals from both preamplifiers connected to the primary detector were summed using a fan-in/fan-out module (model 740, Phillips Scientific, USA) and fed to a constant fraction discriminator (model 454, Canberra, USA) as the input for a time-to-amplitude converter (model 2145, Canberra). The other input to the time-to-amplitude converter came from the secondary detector.

All external radiation sources were removed during the experiments using internal radiation sources. Events were

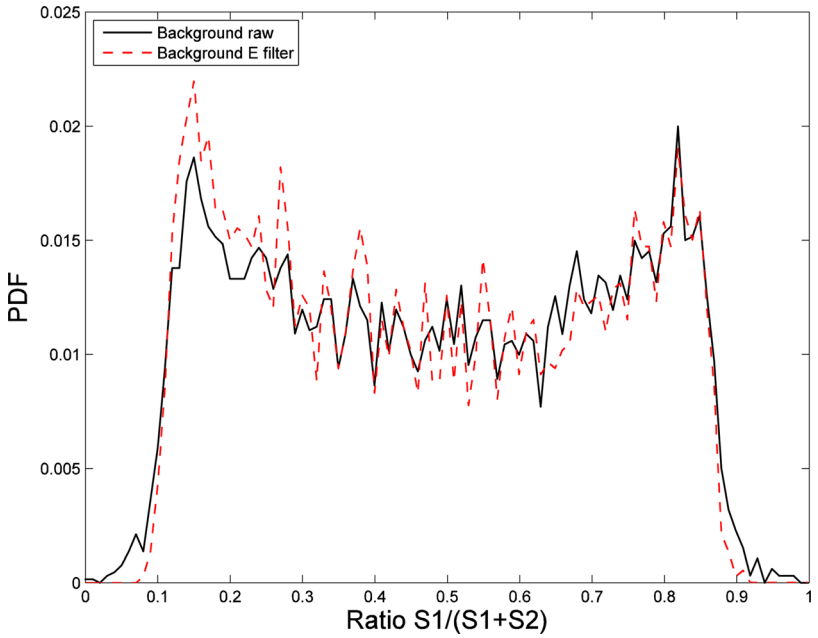

FIG. 3. Distributions of normalized signal ratios measured from internal radiation with and without a 300–650 keV energy filter.

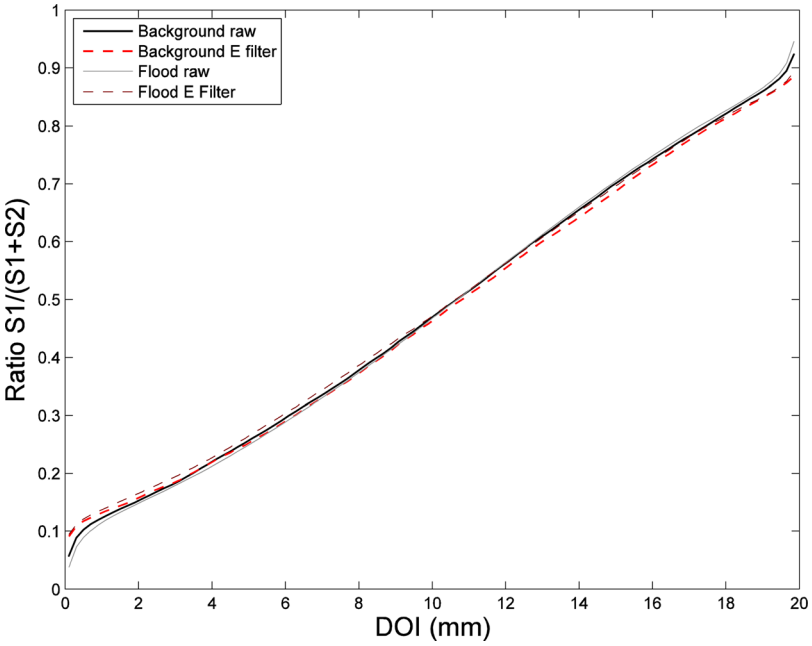

FIG. 4. DOI functions measured from scintillator internal and external uniform flood radiation with and without a 300–650 keV energy filter. The impact of the energy filter was minor except at the scintillator edges, where Compton scattered gamma rays tended to escape.

triggered and acquired when the sum signals from the two SSPMs exceeded the acquisition low-level signal threshold, which was set at the level minimally above the sum signals from the two SSPMs' dark-count noises which corresponded to 50–70 keV depending on the particular crystal, depth, and physical setup.

II.E. Data analysis

DOI function was defined as the relationship between the DOI position (z) and the corresponding ratio of measured signals from two photon sensors for interactions at a specific DOI position. The signal ratio R was defined as,

$$R = \frac{S1}{S1 + S2}, \tag{1}$$

where $S1$ and $S2$ are the signal amplitudes acquired from two SSPMs after electronic amplification.

The distribution of the internal radioactivity in LYSO scintillators is usually uniform across the scintillator depth. If the distribution of detected internal radiation is also uniform across the scintillator depth, then our method of DOI function calibration, which was originally validated with the use of an external uniform flood source, can be simply applied using internal interactions. However, the detected distribution of internal radiation may not be uniform. For example, the detected signal level of 511-keV gamma rays at different depths could be different because of a different amount of scintillation photon surface absorption and scatter along the photon propagation paths. Thus, the detected minimal signal levels for events from different scintillator depths could correspond to different energies, even with the

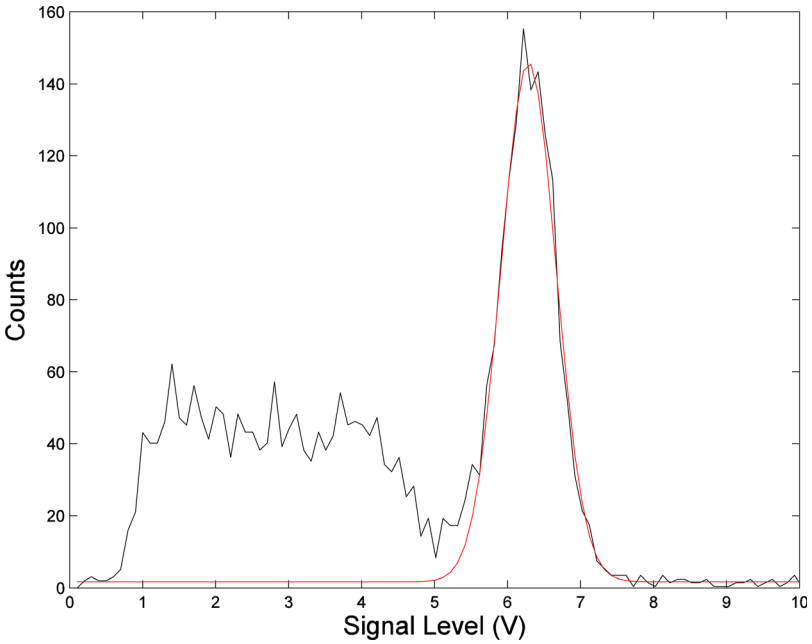

FIG. 5. A typical energy spectrum measured from gamma rays at one DOI position defined by the step-and-shoot method with electronic collimation. A Gaussian function was applied to fit the spectrum. The measured energy resolution was ~14%.

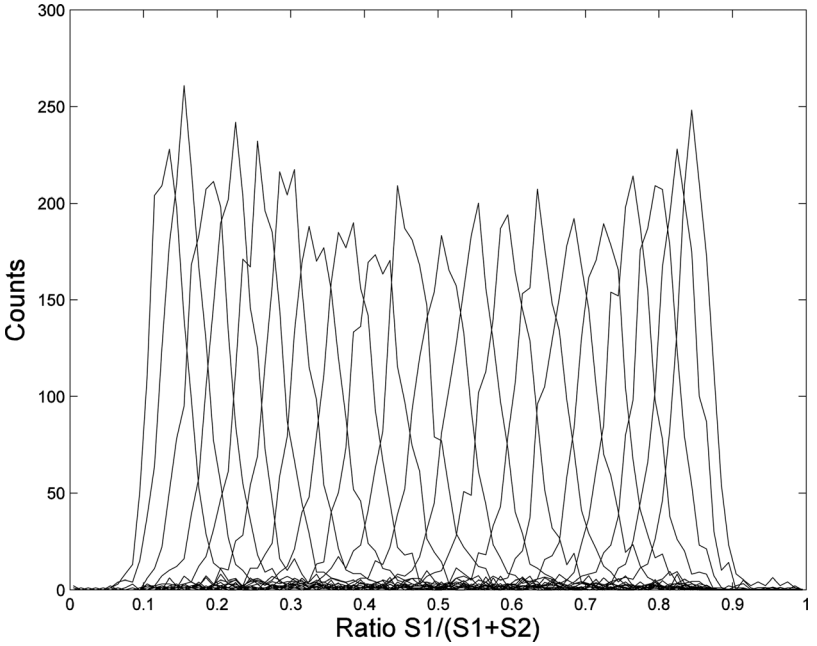

FIG. 6. Distribution of signal ratios measured from different DOI positions with the step-and-shoot method. No energy filters were applied.

same acquisition threshold level. This may lead to a nonuniform distribution of detected internal radiation across the scintillator depth and cause errors in DOI function measurement. In principle, this problem can be solved easily by using a low signal-threshold level for acquiring most internal radiation with minimal event loss, and then by applying the same energy filter (e.g., 300–650 keV) to events from different DOI positions in the postacquisition data process. We evaluate this approach for crystals with rough surface finish.

Other measurements of detector performance from the internal and external radiation sources, including signal level distributions and detected event counts at different DOI positions and resolutions of energy, timing, and DOI were also calculated and compared.

For scintillator array measurements, the x and y position for each event in a crystal map was calculated using a center-of-mass calculation. A crystal was selected with positioning windows placed around its peak position. Once events localized to a particular crystal were selected, analysis was performed on that subset of data, where the subsequent DOI analysis for interactions within each crystal was the same as for the single scintillator measurement.

III. RESULTS

For single scintillator studies, the results measured from three scintillators with representative surface finishes and geometries are described in detail, followed by summary results of all scintillators with different surface finishes and

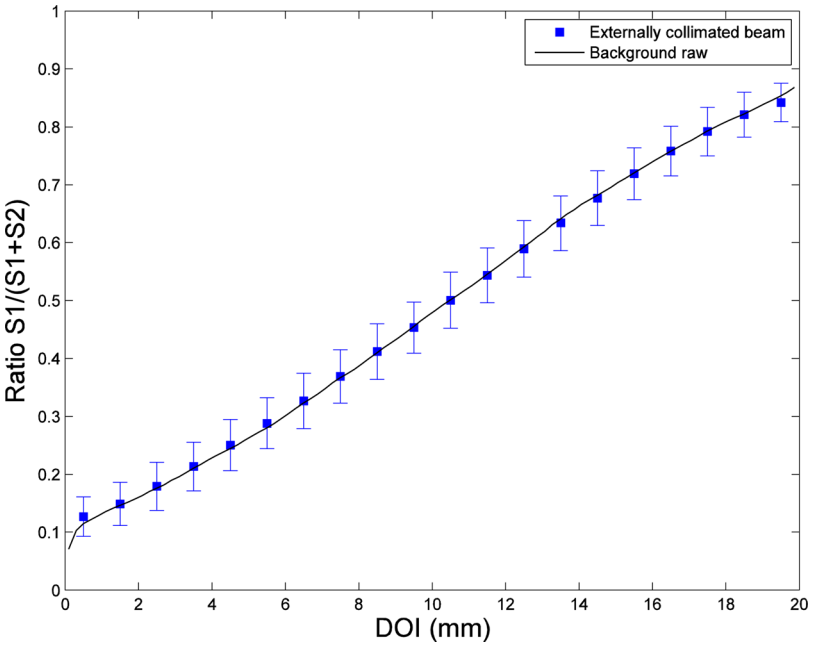

FIG. 7. DOI functions measured from both internal radiation and external radiation with the step-and-shoot method. No energy filters were applied. The agreement between DOI functions was excellent. The error bars were calculated from the Gaussian curve fitting to those distributions of signal ratios shown in Fig. 6.

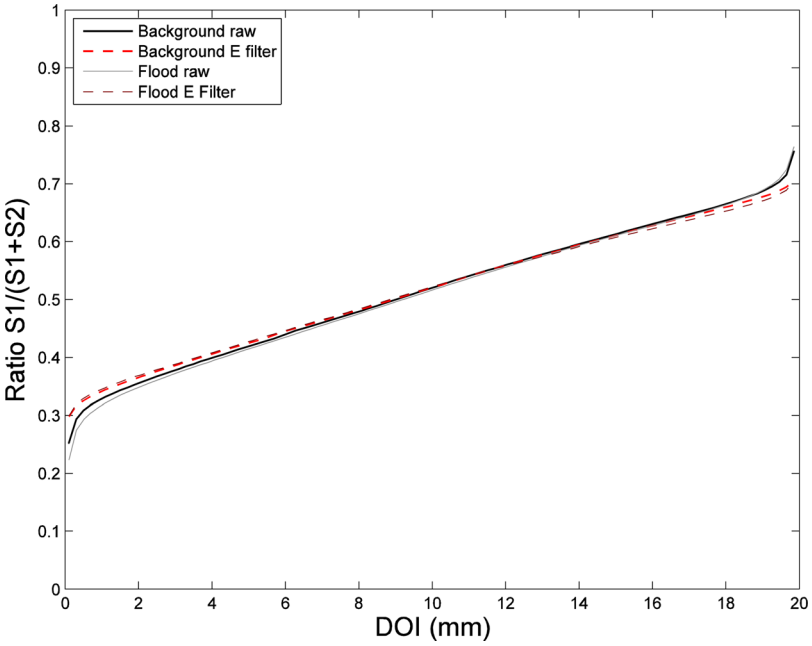

FIG. 8. DOI functions measured from internal radiation and external uniform flood radiation with and without a 300–650 keV energy filter.

geometries. For scintillator array study, the results measured from different methods for crystals at three representative positions inside the array are compared, followed by a summary table.

III.A. $2 \times 2 \times 20$ mm^3 LYSO scintillator with a saw-cut rough surface finish

A typical energy spectrum of scintillator internal radiation measured from one SSPM connected to the primary detector is shown in Fig. 2. The acquisition signal threshold was set just above the noise level. For each internal radiation event, the ratio of signals acquired from both SSPMs was calculated using Eq. (1), with its value ranges from 0.0 to 1.0. The distribution of these signal ratios was normalized by dividing the integration value of this distribution, which is a measured probability density function (PDF) of the signal ratio (Fig. 3). The similar PDF function from an external uniform flood source was also measured. Based on the new DOI function calibration method, DOI functions were calculated with the raw data acquired from both internal and external sources (Fig. 4). With the exception of very minor differences near the crystal edges, the agreement between the two DOI functions was very good. The PDFs measured from the internal radiation and the DOI functions with and without applying an energy filter (300–650 keV) are shown in dashed lines. The energy filter further improved the agreement between the DOI functions measured from the two sources, but the improvement was quite small for a scintillator of this size and surface finish.

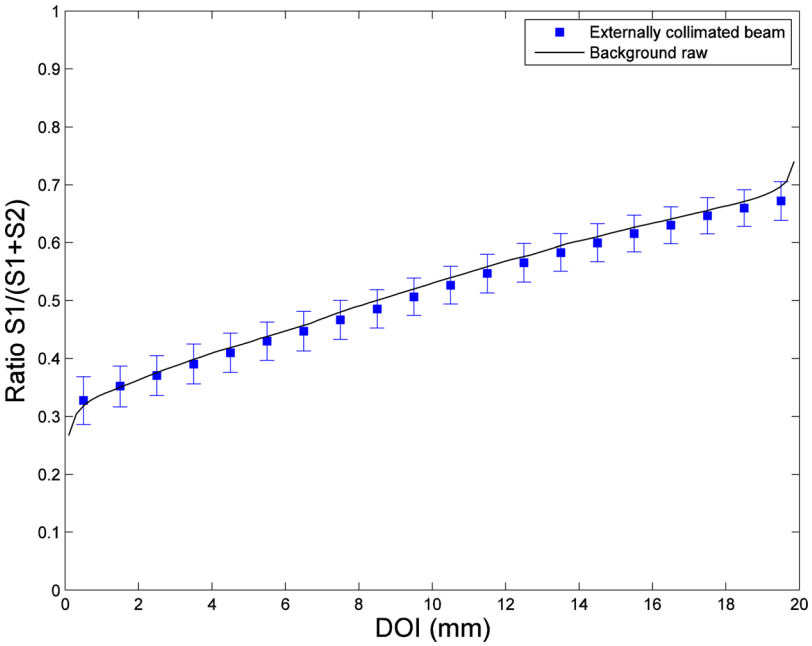

FIG. 9. DOI functions measured from internal radiation and the step-and-shoot method. No energy filter was applied. The slopes of these DOI functions were much smaller than those measured from the scintillator with the same size but rough surface finish, which reflects the strong influence of surface finish has on DOI resolution.

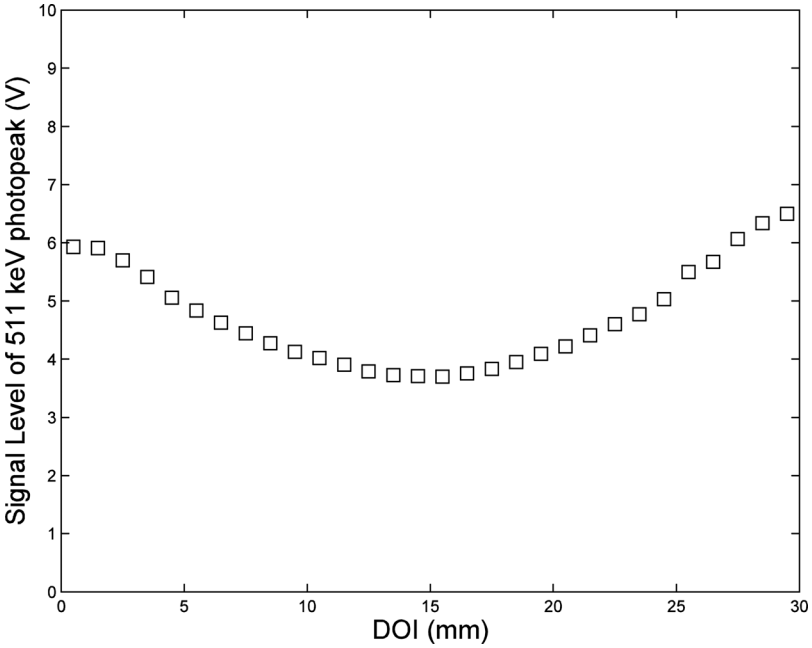

FIG. 10. Distribution of 511-keV signal level with a $1.5 \times 1.5 \times 30$ mm^3 LYSO with rough surface finish. The substantial light loss at the central DOI region reflects the fact that most scintillation photons took long paths to the scintillator ends and underwent severe light loss with the surface absorptions.

To further validate the accuracy of using internal radiation to measure the DOI function, separate data were acquired with the step-and-shoot method. A typical measured energy spectrum and the distribution of signal ratios at different DOI positions are shown in Figs. 5 and 6. The energy and DOI resolutions were around 14% and 2.0 mm, respectively. The agreement between the corresponding DOI function and the DOI function measured from the internal source under the same measurement conditions was excellent (Figs. 4 and 7). The shapes of the DOI functions measured from the internal source in Figs. 4 and 7 are slightly different because these were different measurements taken at different times under different conditions.

Other detector characteristics were also measured using the step-and-shoot method. The measured counts and 511-keV signal level as a function of DOI were uniformly distributed over the DOI with less than 10% variation. The resolutions of coincidence timing, energy, and DOI were also relatively uniform over the DOI. The values of these resolutions are adequate for most PET applications.

III.B. $2 \times 2 \times 20$ mm^3 LYSO scintillator with a 12-μm polished surface finish

The measurements obtained with this scintillator were similar to those of the scintillator described above. The distribution of normalized signal ratios, DOI functions measured with the internal source, the external uniform flood source and the step-and-shoot method are shown in Figs. 8 and 9. There was a signal gain difference between the two channels connected to the primary detector, but this did not affect the DOI or other

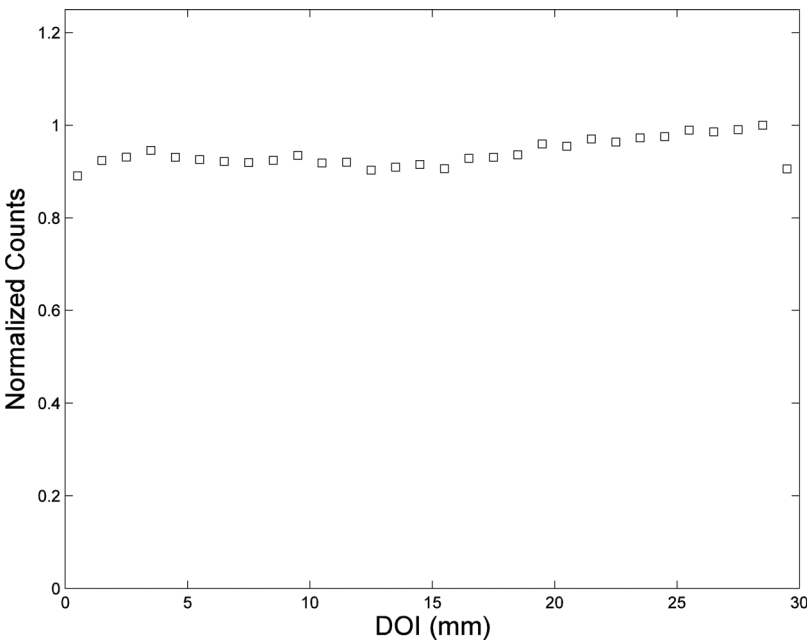

FIG 11. Distribution of counts over DOI positions with the step-and-shoot method by applying minimally low energy threshold. The distribution was still relatively uniform aside from the severe light loss for events that originated in the middle DOI region.

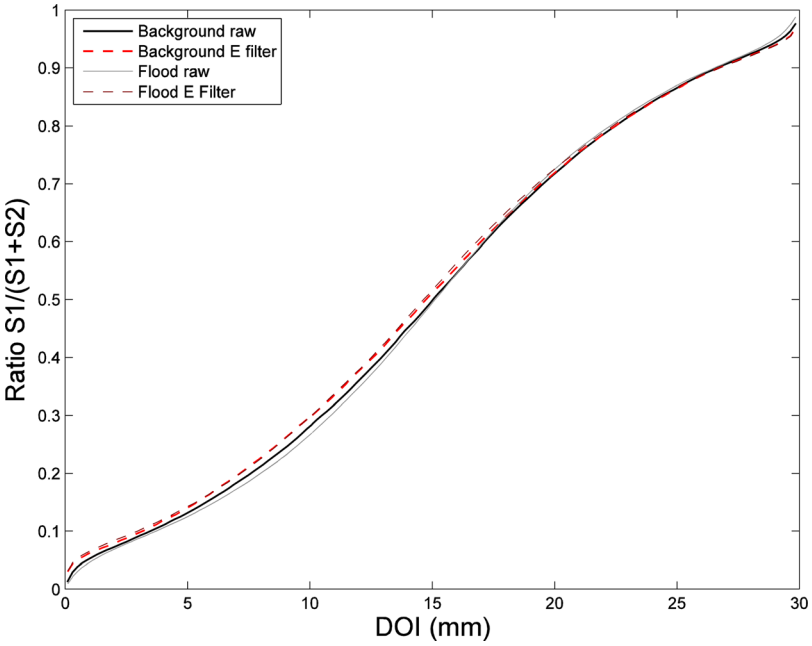

FIG. 12. DOI functions measured from internal radiation and external uniform flood radiation with and without a 300–650 keV energy filter.

performance measurements. The agreement between the DOI functions measured from internal and external radiation sources was also excellent, regardless of whether an energy filter was used. Good uniformities across the DOI were achieved with this scintillator. However, while both the timing and energy resolutions were slightly improved, the DOI resolution worsened, as demonstrated by previous similar studies.[6,9,12]

III.C. 1.5 × 1.5 × 30 mm^3 LYSO scintillator with a saw-cut finish and extensive scintillation light loss

The geometry and rough surface of this scintillator caused scintillation photon absorption and signal loss, in particular for radiation near the middle depth of the scintillator. The signal levels of 511-keV gamma interactions were uneven across the DOI (Fig. 10). By setting the acquisition signal threshold to a minimal level above the noise, the measured count distribution was still relatively uniform across the DOI if the slightly unbalanced gains between the two SSPMs were taken into account. The measured distribution of normalized total counts from the external source is shown in Fig. 11. Although the DOI functions from the internal and external radiation deviated, these deviations were within the measurement uncertainties, and the maximal difference in DOI positions calculated with these different DOI functions was less than 1.0 mm, regardless of whether an energy filter was applied (Figs. 12 and 13).

The other detector performance measurements are shown in Fig. 14. The coincidence timing resolution reaches over 5 ns due to increased light loss, indicating that this scintillator is not suitable for PET applications. Nevertheless, the DOI

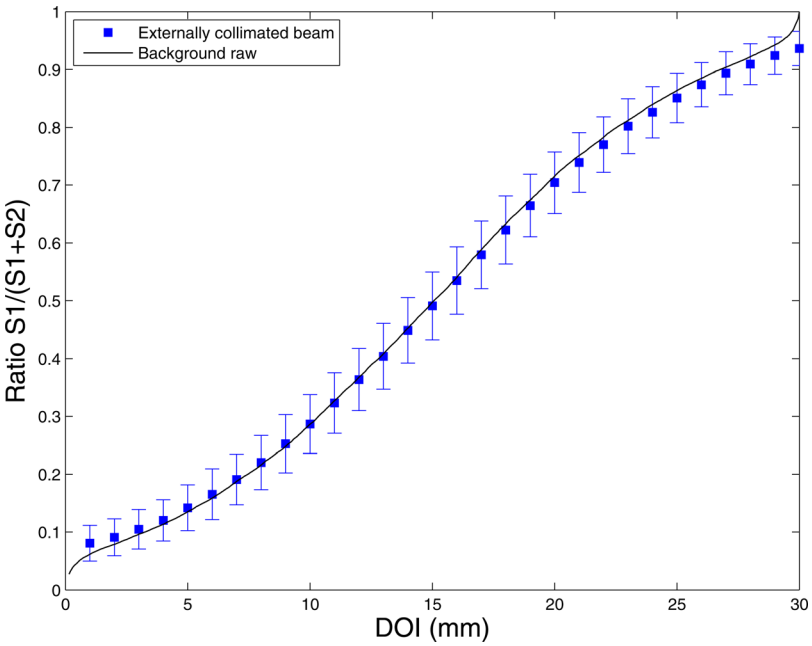

FIG. 13. DOI functions measured from both internal radiation and external radiation with the step-and-shoot method. No energy filters were applied.

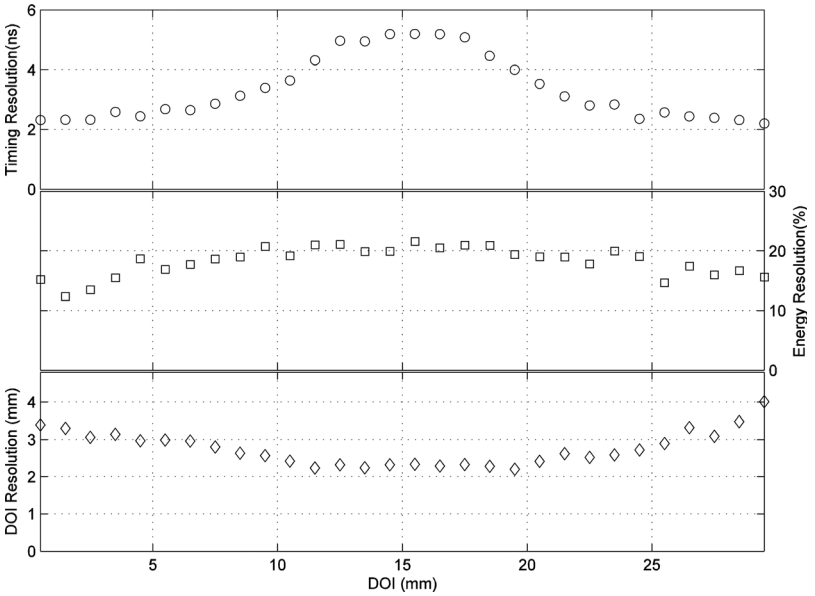

FIG. 14. Resolutions of coincidence timing, energy, and DOI as functions of DOI positions. The values of these resolutions were worse than the corresponding values measured previously with other different scintillator geometries.

functions measured from the internal source still matched consistently with those measured from the external sources, indicating that the DOI function calibration with internal scintillator radioactivity can provide the same accurate DOI function for most scintillator geometries and surface finishes that are suitable for PET applications (Figs. 12 and 13).

III.D. Summary results of all individual scintillators

To further evaluate the accuracy and consistency of different DOI function calibration methods, we evaluated 11 LYSO scintillators with different surface finishes and sizes using internal and external radiation sources. The standard deviations of the 11 LYSO scintillators' differences in DOI positions calculated from different DOI calibration methods are summarized in Table III. The standard deviation of the differences in DOI positions in all scintillators, including those with rough surface finishes and geometries prone to scintillation light loss, ranged from ~0.02 to ~0.63 mm. In general, applying an energy filter improved the agreement between the measurements from the internal source and the measurements of the step-and-shoot method but not the agreement between the measurements of the internal and external uniform flood sources. Nevertheless, the overall standard deviation of the difference among measured DOI positions in all studies were much smaller than 1.0 mm, which demonstrates the accuracy of using internal scintillator radioactivity to calibrate DOI function.

TABLE III. Average DOI difference (standard deviation in mm) of the calibrated depths between different DOI calibration methods for each crystal surface and geometry tested.

	Without energy filter			With energy filter		
	Difference between different DOI calibration methods					
Crystal type	Collimated–internal	Collimated–flood	Flood–internal	Collimated–internal	Collimated–flood	Flood–internal
1.5 × 20 mm rough cut	0.23	0.56	0.69	0.64	0.25	0.78
1.5 × 20 mm 30 μ finish	0.26	0.51	0.67	0.53	0.33	0.76
1.5 × 20 mm 12 μ finish	0.85	0.38	1.00	0.42	0.39	0.29
1.5 × 20 mm 9 μ finish	0.28	0.50	0.63	0.67	0.36	0.92
1.5 × 20 mm 5 μ finish	0.79	0.87	0.13	0.89	0.51	0.44
1.5 × 20 mm 0.5 μ finish	2.45	2.33	0.16	2.56	1.24	1.42
1.5 × 30 mm rough cut	0.25	0.54	0.72	0.55	0.26	0.70
1.5 × 20 mm 30 μ finish	0.30	0.56	0.78	0.30	0.28	0.48
1.5 × 20 mm 12 μ Finish	0.30	0.51	0.72	0.60	0.44	0.89
1.5 × 20 mm 9 μ finish	0.54	0.28	0.75	0.35	0.49	0.73
1.5 × 20 mm 5 μ finish	1.30	0.19	1.21	0.82	0.73	0.37
1.5 × 20 mm 0.5 μ finish	0.92	0.25	0.74	0.19	1.08	1.01
1.5 × 30 mm rough cut	0.53	0.33	0.75	0.35	0.38	0.62
2 × 30 mm rough cut	0.62	0.28	0.76	0.29	0.42	0.54
2 × 40 mm rough cut	0.74	0.69	0.45	1.09	0.35	1.22

III.E. Scintillator array

Fig. 15 shows the crystal map measured from an external flood source, which indicates an excellent crystal identification capability. The difference in DOI functions measured from scintillators with different calibration methods are small, as shown in Fig. 16 from three representative scintillators at the entrance, center and exit side of the array compared to the external source location, and in Table IV for all scintillators at different positions inside the array. The differences between the external uniform flood and internal radiation methods are consistently less than the differences between the collimated radiations and other two methods, which is mainly due to setup uncertainties in the alignment of the beam in the step-and-shot method. Additionally, the alignment between the data with the collimated source method and the data with the flood and internal source methods becomes worse further from the beam entrance. One explanation for this effect is that the inter-crystal scatters make the interaction positions less collimated as the interaction is further from the entrance face. While the flood source also has scatter, the scatter should be fairly uniform, and not degrade the probability distribution function. However, any scatter of the collimated source will cause a mismatch between the R value and the source position. This implies that the mismatch at the exit side of the detector is not a limitation of the calculation based on internal events, but a limitation of collimated pencil beams at depth across a detector. Nevertheless, all these differences are substantially less than 1.0 mm, demonstrating that DOI function of a practical PET detector can be measured from either method. In practice, using internal radioactivity should provide the most convenient and inexpensive method of DOI response function calibration.

IV. DISCUSSION AND CONCLUSION

As we had indicated in the previous study that using internal radioactivity provides a practical, simple, and accurate method for calibrating DOI function without the need for an expensive or complicated external radiation source.[1] The method can be used to calculate any DOI function which can be either linear or nonlinear.

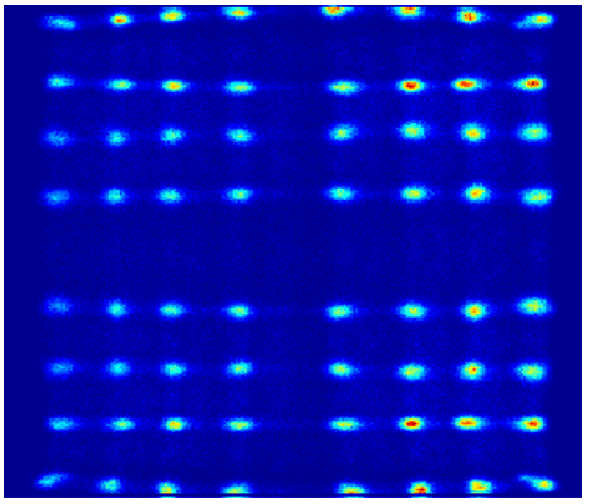

FIG. 15. A crystal map measured from irradiation of a flood source of 511 keV gamma rays. All 64 crystals are well separated.

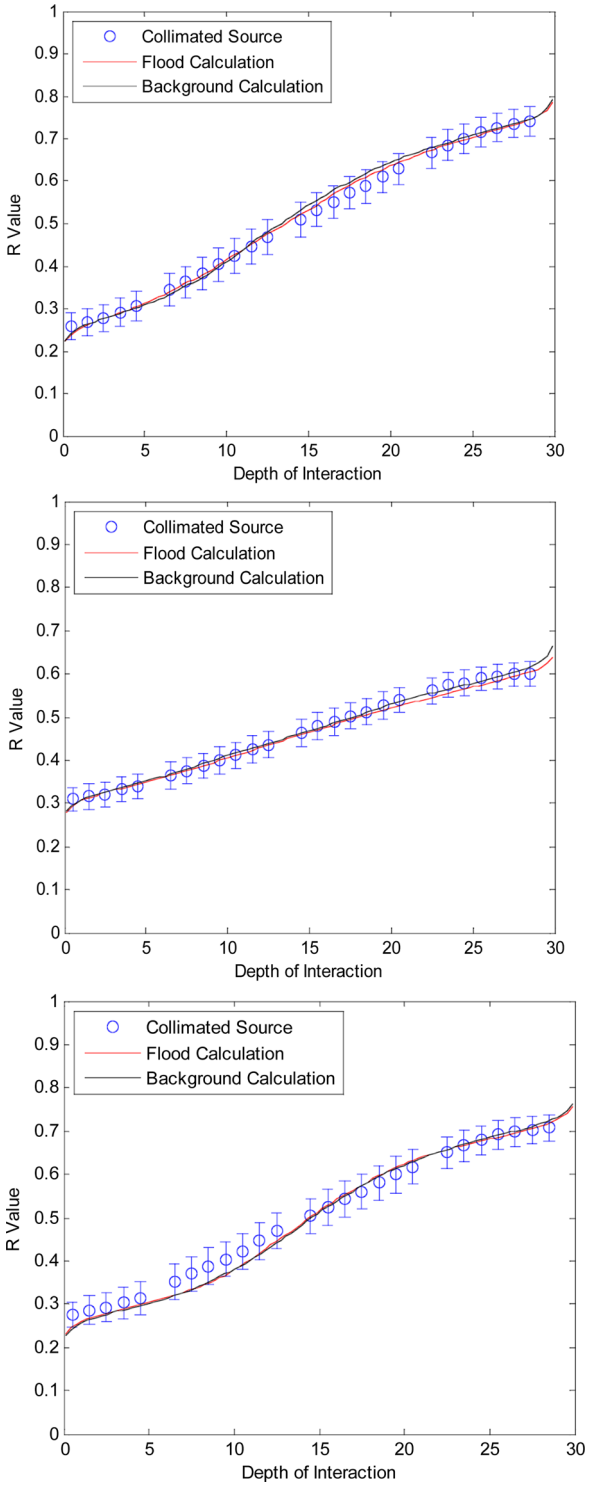

FIG. 16. DOI functions measured from crystals within the array. An electronically collimated Na-22 source was used to select only one row crystals, and DOI functions from three representative crystals were plotted from that row (top to bottom) that correspond to entrance, center and exit crystals from the array side compared to external source location. For all crystals, DOI functions calibrated from different methods align well within the errors of the measurement.

TABLE IV. Average DOI difference (standard deviation in mm) of the calibrated depths between different DOI calibration methods for crystals at different scintillator array positions. The 1st column crystals are closest to the external source, then the 2nd row crystals, and so on.

Crystal column #	1	2	3	4	5	6	7	8
Collimated–flood	0.55	0.61	0.58	0.65	0.69	0.64	0.69	0.64
Collimated–internal	0.58	0.68	0.68	0.64	0.64	0.50	0.64	0.75
Flood–internal	0.22	0.31	0.68	0.71	0.62	0.45	0.48	0.29

We found that although the distribution of original internal radiation positions could be assumed to be uniform across the scintillator depth, the detected events from an internal source may not be uniform across the depth region of a long scintillator with a rough surface. However, this problem can be solved sufficiently to obtain an accurate DOI function by applying a low signal threshold during image acquisition and an energy filter during postacquisition processing. Our study validates this method even in some of the worse case scenarios for a dual-ended-scintillator readout with 50% light loss.

Yang *et al.*[16] have also used internal radioactivity to calculate the DOI functions of an array of LYSO scintillators with dual-ended-scintillator readout. Their method uses a similar data acquisition and process as the one presented in this study except it assumes a linear DOI function. Their model assumes that the two ends of the crystal correspond to R values with half the peak likelihood. Essentially they assume that the edges of the R-space histogram are the two crystal end faces, and the rest of the DOI response function may be estimated with a single line fit through the two edge values. Their model-based method applies well for detectors with linear DOI functions and has the advantage of being insensitive to external source position. While linear DOI function is a good approximation for some detectors, it is common that the DOI functions of different detectors with different surface conditions or even different crystals inside the same detector may not be linear. This is demonstrated in Fig. 16 where the central crystal is well modeled with a linear fit, but the edge crystals are nonlinear. Additionally, in some cases the edge of the detector may not correspond to the half maximum of the probability density function. Therefore, the new method presented in this study, which does not depend on the DOI function shape, can provide more accurate and robust DOI measurement, especially in extreme cases such as array edges.

In summary, we validated that internal scintillator radioactivity can be used to calculate the DOI function with practically the same accuracy as that measured from an external radiation source with either a conventional step-and-shoot method or uniform flood source radiation, for a PET detector with either a single LYSO scintillator or an array of LYSO scintillators. This match holds across various scintillator geometries, surface treatments, for individual crystals, and for crystals at various positions within an array that involve different amounts of light sharing.

ACKNOWLEDGMENTS

The authors thank Drs. Xishan Sun and Allan K. Lan for assisting in experimental setup and Keith Vaigneur from Agile Engineering Inc for providing LYSO scintillator samples. This study was supported by award R21EB007581 from the National Biomedical Imaging and Bioengineering and an Institutional Research Grant (IRG) from The University of Texas MD Anderson Cancer Center.

[a]Author to whom correspondence should be addressed. Electronic mail: yiping.shao@mdanderson.org. Telephone: 713-745-2370; Fax: 713-563-2724.

[1]Y. Shao, R. Yao, and T. Ma, "A novel method to calibrate DOI function of a PET detector with a dual-ended-scintillator readout," Med. Phys. **35**(12), 5829–5840 (2008).
[2]R. Nutt, "Is LSO the future of PET?" Eur. J. Nucl. Med. Mol. Imaging **29**, 1523–1525 (2002).
[3]B. J. Kemp *et al.*, "NEMA NU 2-2001 performance measurements of an LYSO-Based PET/CT system in 2D and 3D acquisition modes," J. Nucl. Med. **47**(12), 1960–1967 (2006).
[4]S. R. Cherry, J. A. Sorenson, and M. E. Phelps, *Physics in Nuclear Medicine*, 3rd ed. (Saunders, Philadelphia, Pennsylvania, 2003).
[5]R. Yao, T. Ma, and Y. Shao, "Lutetium oxyorthosilicate (LSO) intrinsic activity correction and minimal detectable target activity study for SPECT imaging with a LSO-based animal PET scanner," Phys. Med. Biol. **53**(16), 4399–4415 (2008).
[6]W. W. Moses and S. E. Derenzo, "Design studies for a PET detector module using a PIN photodiode to measure depth of interaction," IEEE Trans. Nucl. Sci. **41**(4), 1441–1445 (1994).
[7]Y. Shao, H. Li, and K. Gao, "Initial experimental studies of using solid-state photomultiplier for PET applications," Nucl. Instrum. Methods A **580**, 944–950 (2007).
[8]W. W. Moses *et al.*, "A room temperature LSO/PIN photodiode PET detector module that measures depth of interaction," IEEE Trans. Nucl. Sci. **42**(4), 1085–1089 (1995).
[9]Y. Shao *et al.*, "Dual APD array readout of LSO crystals: optimization of crystal surface treatment," IEEE Trans. Nucl. Sci. **49**(3), 649–654 (2002).
[10]Y. Shao *et al.*, "Design studies of a high resolution PET detector using APD arrays," IEEE Trans. Nucl. Sci. **47**(3), 1051–1057 (2000).
[11]K. C. Burr *et al.*, "Evaluation of a prototype small-animal PET detector with depth-of-interaction encoding," IEEE Trans. Nucl. Sci. **51**(4), 1791–1798 (2004).
[12]Y. Yang *et al.*, "Depth of interaction resolution measurements for a high resolution PET detector using position sensitive avalanche photodiodes," Phys. Med. Biol. **51**, 2131–2142 (2006).
[13]C. Pepin, P. Berard, and R. Lecomte, "Assessment of reflective separator films for small crystal arrays," *IEEE Nuclear Science Symposium Conference Record* (The Institute of Electrical and Electronics Engineers, Inc., Piscataway, NJ, 2001), Vol. **2**, pp. 879–883.
[14]Z. Deng *et al.*, "Development of an eight-channel time-based readout ASIC for PET applications," IEEE Trans. Nucl. Sci. **58**(6), 3112–3218 (2011).
[15]X. Sun *et al.*, "Energy and timing measurement with time-based detctor readout for PET applications: Principle and validation with discrete circuit components," Nucl. Instrum. Methods A **641**, 128–135 (2011).
[16]Y. Yang *et al.*, "Depth of interaction calibration for PET detectors with dual-ended readout by PSAPDs," Phys. Med. Biol. **54**, 433–445 (2009).